

X-Ray Small-Angle Studies of the Pyruvate Dehydrogenase Core Complex from *Escherichia coli* K-12

I. Overall Structure of the Core Complex

Helmut Durchschlag

Institut für Physikalische Chemie der Universität Graz, Austria,
and Biochemie II, Universität Regensburg

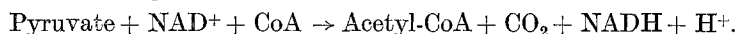
Received January 7, 1974/Accepted February 12, 1975

Abstract. The pyruvate dehydrogenase core complex from *E. coli* K-12, defined as the multienzyme complex which can be obtained with a unique polypeptide chain composition, has been investigated in solution with the X-ray small-angle technique. The molecular mass of the core complex of $3.78 \cdot 10^6$ daltons verifies the ratio of polypeptide chains of 16:16:16 of the three enzyme components, pyruvate dehydrogenase, dihydrolipoamide transacetylase, and dihydrolipoamide dehydrogenase, present in the complex. In connection with the values obtained for the radius of gyration (156.5 Å), volume ($1.07 \cdot 10^7$ Å³) and amount of solvent associated with the complex (1.03 g/g) a loose packing of subunits in the complex has to be assumed. The maximum diameter of the core complex of 433 Å, as determined from the correlation function, corroborates the large extension of the complex. The comparison of experimental and theoretical scattering curves reveals a relatively isometric overall shape of the core complex.

Key words: Correlation Function — Radius of Gyration — Molecular Weight — Volume — Isometric Overall Shape.

Introduction

The pyruvate dehydrogenase complex catalyzes the oxidative decarboxylation of pyruvate according to the overall reaction:



This reaction, proceeding with enzyme bound intermediates, requires three different enzyme components present in the complex (Gunsalus, 1954; Koike *et al.*, 1963): Pyruvate dehydrogenase (enzyme 1, E 1), dihydrolipoamide transacetylase (E 2), and the flavoprotein dihydrolipoamide dehydrogenase (E 3).

It has been established that the polypeptide chains in each component of the *E. coli* K-12 complex are identical; their molecular weights were found to be $M_r, E_1 = 100000$, $M_r, E_2 = 80000$, $M_r, E_3 = 56000$ (Vogel *et al.*, 1971; Vogel and Henning, 1971, 1973). Similar molecular weights were reported for the *E. coli* Crookes complex (Perham and Thomas, 1971; Eley *et al.*, 1972). Possible distributions of the *E. coli* Crookes pyruvate dehydrogenase and flavoprotein chains around the transacetylase core are discussed by Reed and co-workers (Reed and Oliver, 1968; Eley *et al.*, 1972).

Enzymes: Pyruvate dehydrogenase complex = pyruvate dehydrogenase (EC 1.2.4.1) plus dihydrolipoamide transacetylase (EC 2.3.1.12) plus dihydrolipoamide dehydrogenase (EC 1.6.4.3).

As has been shown recently (Vogel *et al.*, 1972a, b; Henning *et al.*, 1972), the amount of pyruvate dehydrogenase present in the *E. coli* K-12 complex can vary. A complex can be isolated which reproducibly has a unique polypeptide chain composition. From this complex, which Henning and associates have called "core complex", excess pyruvate dehydrogenase has been removed by chromatography on calcium phosphate gel. This removal did not result in a significant loss in overall activity. The physiological significance of this "excess" enzyme is unknown till today. For the core complex, which can also be produced *in vivo*, the authors measured a ratio of the polypeptide chains of the enzyme components of 1:1:1, with a total of 48 chains. Independent evidence for this number of chains was obtained by determination of the FAD content of the enzyme complex. In the pyruvate dehydrogenase complex from which excess pyruvate dehydrogenase has not been removed, the polypeptide chain ratio was found to be 1.35:1:1. The findings of Henning and co-workers clearly indicate that the arrangement of polypeptide chains in the transacetylase component and the enzyme complex from *E. coli* K-12 must be other than that of the *E. coli* Crookes complex, for which a chain ratio of 2:2:1 was reported (Eley *et al.*, 1972). The difference between these two complexes was also pointed out by Dennert and Höglund (1970) by a comparison of diverse molecular parameters of both complexes, such as electrophoretic mobility, isoelectric point, or sedimentation constant.

In this paper the X-ray small-angle diffraction technique (*cf.* Kratky, 1963; Kratky and Pilz, 1972) has been used as a further and independent method for measuring size, shape and structure of the pyruvate dehydrogenase core complex from *E. coli* K-12 in solution. Furthermore the method should prove especially reliable in determining the exact value of the molecular weight of the core complex, thus establishing the ratio of polypeptide chains present in the core complex.

Preliminary reports have been presented (Durchschlag, 1973, 1974).

Experimental Procedure

Preparation of the Enzyme Complex

Pyruvate dehydrogenase complex was prepared from the K-12 strain YMel and the regulatory mutants K1-1 LR8-13 and K1-1 LR8-16 which synthesize the enzyme complex constitutively (Flatgaard *et al.*, 1971). Growth conditions, purification procedure, enzyme assays, sources of reagents, etc., have been described in detail by Vogel *et al.* (1971, 1972a). As mentioned above, the core complex is the enzyme complex from which excess pyruvate dehydrogenase component had been removed during chromatography on calcium phosphate gel. It is the complex which loses no further components upon rechromatography on this gel.

Enzymatic activity of the complex was measured according to Reed *et al.* (1958). Protein concentrations were measured either by amino acid analyses or by the biuret method (Beisenherz *et al.*, 1953) using a biuret factor determined for the pyruvate dehydrogenase complex (Vogel *et al.*, 1972a).

Enzyme solutions for small-angle measurements were dialyzed at 4° C against 0.1 M potassium phosphate buffer pH 7.0 containing 10⁻³ M EDTA and 10⁻² M 2-mercaptoethanol. Dialysis buffer was used for diluting the enzyme and for the

scattering measurement of the blank solution. Small-angle experiments, carried out twice on enzyme samples prepared independently of each other, yielded a completely identical course of the scattering curves and therefore identical results.

X-Ray Small-Angle Scattering

A stabilized high power X-ray generator with a tube with copper target delivered a sufficiently high primary intensity (50 kV and 30 mA). By means of an air-conditioning system it was possible to maintain a room temperature of $21 \pm 0.5^\circ \text{C}$ and a relative humidity of $60 \pm 5\%$. A closed water circuit system for the X-ray tube took care of constant thermal conditions. A Kratky-camera (Kratky, 1954, 1967; Kratky and Skala, 1958) with a collimation system made of tungsten, practically free from parasitic scattering, was adjusted on the broad side of the line focus. Employing an "opening beam" it was possible to obtain a sufficiently long primary beam with very even intensity distribution (Kratky *et al.*, 1960).

For recording, a proportional counter was used in connection with a pulse-height discriminator focused on the $\text{Cu } K_\alpha$ line (1.54 \AA). The elimination of the influence of the $\text{Cu } K_\beta$ line (1.39 \AA) was carried out by a mathematical procedure (Zipper, 1969).

An improved programmable electronic step scanning device (Leopold, 1968) allowed a fully automatized operation which also includes the possibility of a repeated scanning of the scattering curves. Hereby it could be unequivocally proved that no changes of the sample whatsoever, *viz.* shape, molecular weight, *etc.* occurred during measurement (for instance caused by X-ray irradiation). In addition, enzyme activity before and after X-ray irradiation was routinely checked. Hereby a decrease in enzymatic activity was never detected.

The measurement of the absolute intensity, that is to say, the ratio of the scattered intensity to that of the primary beam, was carried out by the use of a polyethylene platelet as standard sample (Kratky *et al.*, 1966; Pilz and Kratky, 1967; Pilz, 1969).

The solutions were investigated in Mark capillaries and were thermostated to 5.5°C in a cell by means of a Peltier element (Leopold, 1969).

Measurements were carried out down to an angle as small as $9.35 \cdot 10^{-4} \text{ rad}$ (corresponding to a Bragg's spacing of 1650 \AA) which forced the use of a 40μ entrance slit for the innermost part. At somewhat larger angles an entrance slit of 120μ was used to obtain a higher scattered intensity. At each point $3.2 \cdot 10^5$ or $8 \cdot 10^4$ counts were registered for the outer and inner part respectively. This corresponds to a mean statistical error of 0.177 and 0.354%, respectively. For the two ranges measured with different entrance slits a sufficiently long range of overlap was registered.

The proper scattering curve of dissolved molecules was obtained by subtracting the blank curve (originating from the scattering of pure solvent and capillary) from the measured scattering curve of the solution. The curves thus obtained were at first smoothed by hand.

All experimental scattering curves are, as a result of the line-shaped nature of the primary beam cross-section, subject to collimation errors. The collimation errors caused by the finite width and length of the primary beam were eliminated

consecutively according to the mathematical procedures given by Kratky *et al.* (1960) and Guinier and Fournet (1947), respectively. This "slit desmearing" was facilitated by computer programs developed in the Graz Institute (Heine and Roppert, 1962; Heine, 1963; Zipper, 1972).

The specific volume of the enzyme core complex was measured by means of a digital densitometer (Kratky *et al.*, 1969), which was calibrated at 5.5° C using dry nitrogen and water as standards.

Results and Discussion

The result of an X-ray small-angle experiment is a scattering curve, strictly speaking the scattering intensity as a function of the scattering angle. All the information is inherent in this one curve. By means of a consolidated theory and suitable mathematical operations parameters like radius of gyration, molecular weight, volume *etc.* can be derived from the scattering curve. The same quantities can be obtained by using not the scattering intensity itself but its Fourier transformed function, the so-called correlation function. A necessary requirement for the Fourier transformation is a high accuracy of the scattering curve. But, of course, the correlation function does not yield more information than the scattering intensity, but sometimes it is useful to have some controls and advantages in the evaluation, *e.g.* for determination of the maximum diameter of the particle. Additional information about the shape of the particle as a whole can be obtained by comparing experimental and theoretical scattering curves.

The Scattering Curve

In order to eliminate the influence of interparticular interferences upon the scattering curves, the curves were measured at several different protein concentrations ranging from 2.5 to 40 mg/ml. The scattering curve of the enzyme core complex, desmeared, monochromatized and extrapolated to concentration zero is shown in Fig. 1 in a plot of scattering intensity $\phi(h)$ vs. angular argument h . $\phi(h)$ is the scattering intensity standardized to 1 for $h = 0$, and h is related to the scattering angle 2θ and the wavelength λ of the primary beam as follows: $h = (4\pi \sin \theta)/\lambda$. An enlarged presentation of the outer section of the scattering curve shows the appearance of three submaxima, the first and second well defined, the third not very distinct. The first, "isometric" submaximum (at $h = 0.029 \text{ \AA}^{-1}$) possesses an intensity of approximately 1.09% of the main maximum. The scattering curve shows minima, but no zeros.

These plots clearly reveal some characteristics of the experimental scattering curve of the enzyme core complex. After a steep descent of the scattering curve at small angles follows with a short transition range in between a very long outer part of the scattering curve with a relatively high intensity extending to large angles (extending to $h = 0.39 \text{ \AA}^{-1}$).

The steep descent of the scattering curve at small angles can be explained by the high molecular weight of the multienzyme complex, the extension of the scattering curve to large angles by the arrangement of the molecule from subunits. The high intensity in the range of the submaxima indicates a hollow body or at least hollow ranges within the molecule. The occurrence of minima instead of

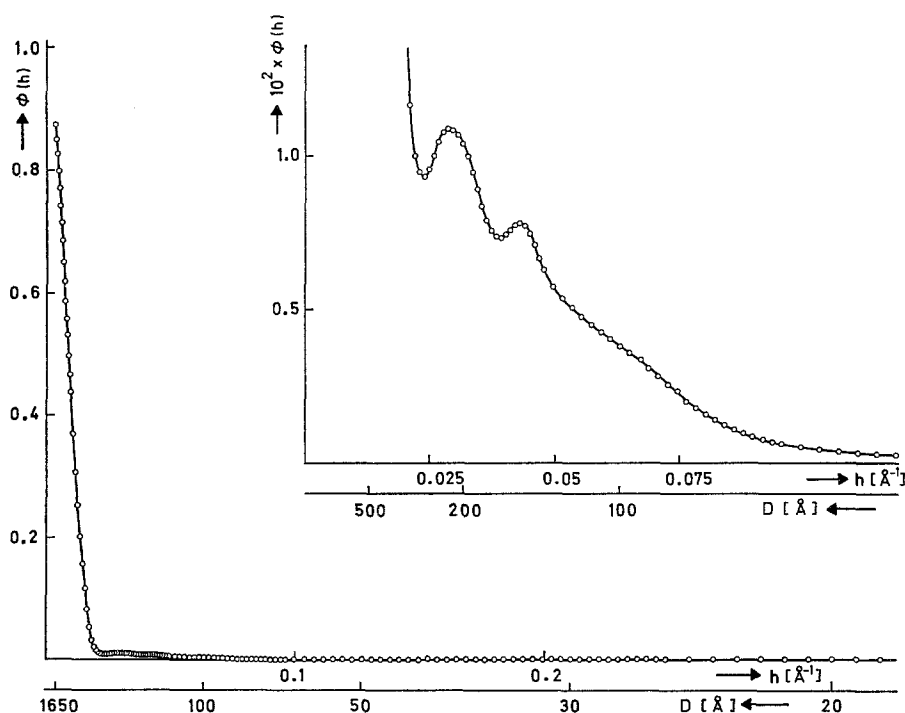


Fig. 1. Scattering curve of the enzyme core complex in a plot scattering intensity $\phi(h)$ vs. angular argument h , desmeared, monochromatized and extrapolated to concentration zero. $\phi(h) = I(h)/I_0$, i.e. scattering intensity standardized to 1 for $h = 0$, where $h = (4\pi \sin\theta)/\lambda$ in \AA^{-1} ; D is the Bragg's spacing in \AA , calculated from $\lambda = 2D \sin\theta$

zeros descloses slightly disturbed spherical symmetry of the complex and is also mainly due to the arrangement of the complex from subunits.

According to Porod (1951, 1952) the intensity in the tail-end of every small-angle scattering curve of a two-phase system from which the collimation error has not been removed follows a course obeying $(2\theta)^{-3}$, and is proportional to $(2\theta)^{-4}$ in the desmeared scattering curve respectively.

Fig. 2 shows the asymptotic trend of the desmeared experimental scattering curve in a plot of $I(2\theta) \cdot (2\theta)^4$ vs. $(2\theta)^4$. The ordinate section of the straight line represents the tail-end constant k_1 which will be used later on, e.g. for determination of the invariant. A constant scattering background, caused by fluctuations in the electron density within the scattering particles (Luzzati *et al.*, 1961), has already been removed during the desmearing procedure.

The Correlation Function

The scattering of a system with statistically varying electron density is characterized by the correlation function $H(x)$ (Debye and Bueche, 1949; Porod, 1951, 1952, 1967; Kirste and Porod, 1962). This function is a measure for interference interaction of two arbitrarily chosen points at a distance x from each

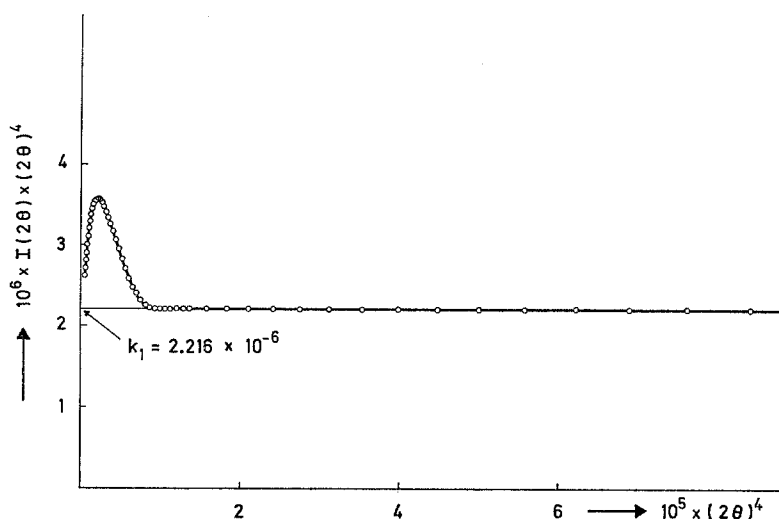


Fig. 2. Plot of $I(2\theta) \cdot (2\theta)^4$ vs. $(2\theta)^4$ of the desmeared scattering curve of the enzyme core complex for evaluation of the tail-end constant k_1 . $I(2\theta)$ is the intensity of the scattering curve in arbitrary units; (2θ) is the whole scattering angle in rad

other; it may be imagined as a probability distribution in space. The correlation function is only in a finite range different from zero, *i.e.* points sufficiently far from each other do not show any correlation in the sense that emitted scattering waves no longer act coherently. Some average quantities may be defined, by taking the integral in one, two, three dimensions respectively:

$$l_c = 2 \int_0^{\infty} H(x) dx \quad (1)$$

$$a_c = 2\pi \int_0^{\infty} H(x) \cdot x dx \quad (2)$$

$$v_c = 4\pi \int_0^{\infty} H(x) \cdot x^2 dx, \quad (3)$$

where l_c = coherence length, a_c = coherence area, v_c = coherence or correlation volume (for a single homogeneous particle v_c is identical with the volume V).

The correlation function $H(x)$ can be obtained by a Fourier transformation of the scattered intensity $I(h)$.

$$H(x) = \frac{k}{2\pi^2} \int_0^{\infty} I(h) \cdot h^2 \frac{\sin hx}{hx} dh, \quad k = \frac{a^2 M}{T_e N P_0 c_2 b V \bar{\rho}^2}, \quad (4)$$

where $\bar{\rho}^2$ = mean square fluctuation of the electron density ($e^2/\text{\AA}^6$).

Maximum Diameter of the Particle

According to the definition of the correlation function, knowledge of it supplies a simple and unconditionally applicable procedure for determining the maximum

diameter of the particle. The correlation function $H(x)$ becomes zero for all distances larger than the maximum diameter of the particle.

Strictly speaking, by means of model calculations on a variety of molecules it turned out that a distance somewhat smaller than the distance between the two utmost points of the particle has to be expected. Obviously, a certain number of "maximum" distances has to be present to show a noticeable scattering effect representing this maximum diameter of the molecule. Nevertheless, this definition of the maximum diameter is a useful operational quantity, probably more useful than the distance between the two utmost points of the particle.

The maximum diameter of the pyruvate dehydrogenase core complex from *E. coli* K-12 was found to be 433 Å. This value is in reasonable agreement with the approximate value of 400 Å estimated by Dennert and Höglund (1970) from electron microscope studies on the *E. coli* K-12 complex. On the other hand, Reed and Oliver (1968) mention a maximum diameter of 300 Å (!) for the complex from *E. coli* Crookes, and a value of 400 to 450 Å for the mammalian pyruvate dehydrogenase complex.

Radius of Gyration

The determination of the radius of gyration of dissolved particles can be performed according to some different methods:

1. The procedure commonly applied makes use of the Guinier approximation. According to Guinier (1939), the intensity scattered at very small angles may be represented by a Gaussian curve:

$$I(2\theta) = I_0 \cdot e^{-KR^2\theta^2}, \quad K = 16\pi^2/3\lambda^2. \quad (5)$$

The radius of gyration R is obtained from the initial slope of the scattering curve in a plot $\log I(2\theta)$ vs. $(2\theta)^2$ (Guinier plot) according to the relation:

$$R = k \sqrt{-\left(\frac{d \log I(2\theta)}{d(2\theta)^2}\right)_{2\theta \rightarrow 0}}, \quad k = \frac{\lambda}{2\pi} \cdot \sqrt{\frac{3}{\log e}} = 0.644 \text{ Å}. \quad (6)$$

Linear extrapolation to scattering angle zero gives the scattering intensity at zero angle. This so-called zero intensity I_0 is directly proportional to the molar mass M (cf. section on Molecular Weight). In consequence of the interparticle interferences both zero intensity and radius of gyration have to be extrapolated to zero concentration.

A slight uncertainty with this method of determining the radius of gyration from the Guinier approximation is given by the fact, that only the innermost points of the scattering curve are used for determining the slope and thereby the radius of gyration. Falsifications of results are more likely, when deviations from the Guinier straight line upward (with anisometric bodies) or downward (with hollow bodies) even at very small angles are to be expected. From the reciprocity of particle size and angular range of scattered intensity follows, that this especially holds true for particles of very large extension. In principle, the same uncertainty is valid for the determination of zero intensity. But here it turned out in practice, that the uncertainty in I_0 is less pronounced (probably due to the smoothing procedure).

Fig. 3 shows the scattering curves of the enzyme core complex at different concentrations in a Guinier plot. After extrapolation to zero concentration (Fig. 4)

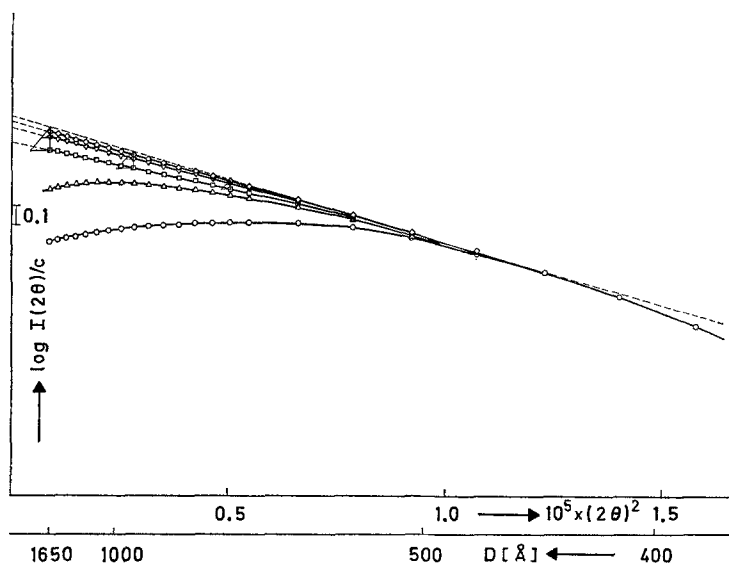


Fig. 3. Guinier-plot of scattering curves at different concentrations. (\circ) $c = 39.4$ mg/ml, (Δ) $c/2$, (\square) $c/4$, (∇) $c/8$, (\diamond) $c/16$, upper dashed line: $c = 0$

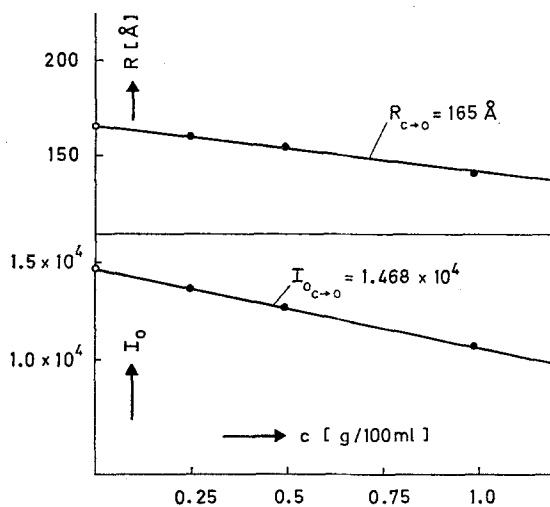


Fig. 4. Concentration dependence of the apparent values of the radius of gyration (above) and zero intensity (below) obtained from the Guinier-plot

the radius of gyration was ascertained to be 165 \AA . The deviation of the experimental scattering curve downward from the Guinier straight line (*cf.* Fig. 3) again indicates hollow parts in the enzyme core complex. According to that what has been mentioned above, it is clear that this downward deflection causes a too high value for the slope, and thus the same for R .

2. Another possibility to determine the radius of gyration makes use of the correlation function $H(x)$. The radius of gyration also of densely packed systems can then be obtained from the relation (Porod, 1951):

$$2R^2 = \frac{\int_0^\infty H(x) \cdot x^4 dx}{\int_0^\infty H(x) \cdot x^2 dx} \quad (7)$$

An obvious advantage of this procedure is the fact, that — in contrary to the Guinier method — the whole scattering curve will be used for determining R (in practice the integration was not extended to ∞ but was terminated at a distance equal to the maximum diameter of the particle). It is evident that the procedure now is much less subject to errors because some of the errors cancel out.

Model calculations of scattering curves of bodies built up from a large number of subunits, and thereby forming cavities within the molecule, have shown, that the radius of gyration obtained from the slope in the angular range accessible to experimental evaluation according to the treatment of Guinier, was some per cent too high. On the other hand, the Fourier transformation of the scattering intensity and calculation according to Eq. (7) allowed a very accurate determination of R .

The value for the radius of gyration of the enzyme core complex obtained from the correlation function was $R = 156.5 \text{ \AA}$. As we had expected, this value for R lies some per cent below that from the Guinier approximation. In the light of the above considerations it is apparent that the value for the radius of gyration obtained from the correlation function is the more reliable.

3. Furthermore, the position of the first (isometric) submaximum can be used for roughly estimating the radius of gyration. For all bodies, the shape of which does not deviate very much from a sphere or a cube, there holds (Mittelbach, 1964)

$$R = \frac{4.5}{h}, \quad \text{where } h = (4 \pi \sin \theta) / \lambda \quad (8)$$

The good accordance between the experimental value for R of 155 \AA , as obtained from the isometric submaximum, and the value obtained from $H(x)$ additionally confirms qualitatively the above stated remarks on the radius of gyration.

Molecular Weight

The molecular weight can be evaluated if primary energy and zero intensity, the latter obtained from the Guinier plot, are known (Kratky *et al.*, 1951; Kratky, 1963, 1964).

$$M = k \cdot \frac{I_0}{P_0} \cdot \frac{a^2}{b c_2 (z_2 - v'_2 \rho_1)^2}, \quad k = \frac{1}{T_e N} = 21.0 \text{ moles/cm}^2, \quad (9)$$

where M = molar mass (g/mol), I_0 = zero intensity [erg/(s · cm²)], P_0 = primary energy per time unit (erg/s), a = distance between sample and plane of registration (cm), b = thickness of sample (cm), c_2 = concentration of sample (g/cm³), z_2 = number of moles of electrons per gram dissolved substance, v'_2 = its isopotential specific volume (cm³/g); in practice, without great error the apparent isopotential specific volume ϕ'_2 (*cf.* Kupke, 1972) can be used instead of v'_2 , ρ_1 = electron density of solvent in moles of electrons per cm³ of solvent, $T_e = 7.90 \cdot 10^{-26} \text{ cm}^2$, Thomson scattering constant of a free electron, and N = Avogadro's number (mol⁻¹).

With the above Eq. (9) and the experimental value at 5.5° C for $\phi'_2 = 0.696$ cm³/g, the calculated molar mass of the enzyme core complex is $M = 3.78 \cdot 10^6$ g/mol. Errors in M could be eliminated largely by using the same enzyme solution for the X-ray experiment (*i.e.* determination of I_0) and the determination of ϕ'_2 and c_2 . The remaining unavoidable errors in M are then mainly due to an uncorrect extrapolation of the Guinier straight line and errors in concentration.

The value for M is in best agreement with the value of $M = 3.75 \cdot 10^6$ g/mol (based on the same ϕ'_2 -measurement), obtained from ultracentrifugal experiments *via* determination of s and D of the core complex from *E. coli* K-12 by Henning and co-workers (Vogel *et al.*, 1972a, b; Henning *et al.*, 1972). At the same time this accordance is also an indirect confirmation of the value for ϕ'_2 , because the value for M is influenced by it in a different way in the techniques of ultracentrifugation or small-angle scattering (*e.g.* a hypothetical specific volume of 0.735 cm³/g would yield $M = 4.32 \cdot 10^6$ g/mol, calculated from s and D , or $M = 5.25 \cdot 10^6$ g/mol, calculated from small-angle scattering data).

The experimentally found value for the molecular weight of $M_r = 3.78 \cdot 10^6$ also agrees with the theoretical value of $M_r = 3.776 \cdot 10^6$, calculated from the molecular weights of the enzyme species for a ratio of polypeptide chains of 16:16:16 postulated by Henning and associates. Hence it follows, that the molecular weight of the complex from *E. coli* K-12, from which excess pyruvate dehydrogenase has not been removed (1.35:1:1 complex with an approximate chain ratio of 22:16:16) should be about $4.4 \cdot 10^6$. There seems also to be good correspondence between this value and that obtained for the *E. coli* Crookes enzyme complex (chain ratio 24:24:12) of $4.6 \cdot 10^6$ based on a partial specific volume of 0.735 cm³/g (Eley *et al.*, 1972).

On the other side, the low molecular weight of $M_r = 3.0 \cdot 10^6$, found by Dennert and Höglund (1970) for the *E. coli* K-12 complex, may be due to a decrease of actual protein concentration caused by the centrifugation procedure preceding their light scattering experiments, as suspected by Vogel *et al.* (1972a). But apart from these light scattering investigations, a comparison of the s -values of the data by Vogel *et al.* (1972a) of $s_{20,w}^0 = 54$ S (after having converted their $s_{5.5,s}^0 = 35.6$ S to standard conditions) and of $s_{20,w}^0 = 53.5$ S by Dennert and Höglund (1970) discloses that these latter authors also investigated something like a "core complex" in their experiments.

Using the data for s , M_r and ϕ'_2 , a frictional ratio of the core complex of $f/f_0 = 1.8$ can be calculated. In conjunction with the data derived later on, this high value for f/f_0 may also be attributed to the open structure of the core complex.

Volume

A relation given by Porod (1951, 1952) allows the absolute determination of the volume of the particles of the disperse phase of the system. Hereby the molecules are assumed to be entirely homogeneous.

$$V_{\text{exp}} = 4 \pi \int_0^{\infty} H(x) \cdot x^2 dx = k \cdot \frac{I_0}{Q}, \quad k = \frac{\lambda^3}{4 \pi} = 0.291 \text{ \AA}^3, \quad (10)$$

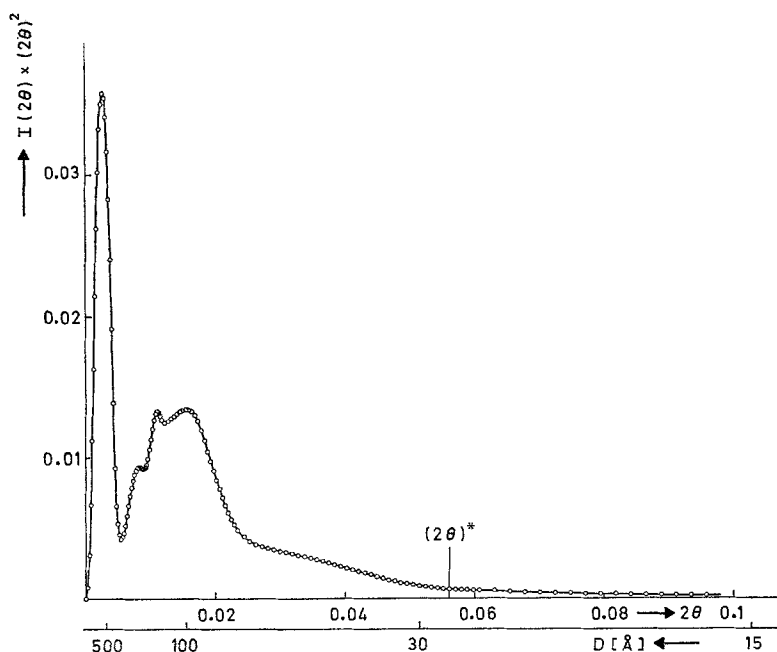


Fig. 5. Plot of $I(2\theta) \cdot (2\theta)^2$ vs. (2θ) for evaluation of the invariant $Q = \int_0^{\infty} I(2\theta) \cdot (2\theta)^2 d(2\theta)$ (for details see text)

$$Q = \int_0^{\infty} I(2\theta) \cdot (2\theta)^2 d(2\theta) = \int_0^{(2\theta)^*} I(2\theta) \cdot (2\theta)^2 d(2\theta) + \frac{k_1}{(2\theta)^*}. \quad (11)$$

The value for the invariant Q (cf. Fig. 5) can easily be ascertained by determining the integral in Eq. (11) up to an optional scattering angle $(2\theta)^*$ in the outer part of the scattering curve numerically (e.g. by Simpson's rule), the rest of the integral up to the angle ∞ analytically by means of the tail-end constant k_1 .

This kind of determining the volume of particles is restricted by the validity of Porod's rule of the $(2\theta)^{-4}$ behaviour in the tail-end of the scattering curve, by the background assumed and the resolution obtained, as well as by deviations from complete homogeneity of the particle. On the other side, the volume of a macromolecule with its complicated tertiary structure is not a well defined quantity. Notwithstanding these restrictions, in a lot of small-angle investigations the volume in the sense defined above turned out to be a useful operational quantity (cf. Durchschlag *et al.*, 1971; Sloan and Velick, 1973).

Using the value for the invariant we obtain a volume $V_{\text{exp}} = 1.075 \cdot 10^7 \text{ \AA}^3$ for the enzyme core complex. This value is in good agreement with $V_{\text{exp}} = 1.043 \cdot 10^7 \text{ \AA}^3$ obtained from $\int_0^{\infty} H(x) \cdot x^2 dx = 8.30 \cdot 10^5 \text{ \AA}^3$. At the same time this accordance shows a high accuracy of the scattering curve and thus of the Fourier transformation of $I(h)$ (cf. Porod, 1967).

The quotient q of experimental volume of dissolved particles V_{exp} and dry volume V_{calc} , as calculated from M and \bar{v}_2 , gives indications for the inner solvation of the complex:

$$q = \frac{V_{\text{exp}}}{V_{\text{calc}}}, \quad V_{\text{calc}} = \frac{M \bar{v}_2}{N}, \quad (12)$$

hence the weight fraction x of solvent per gram of dissolved protein can be calculated:

$$x = \bar{v}_2 d_1 (q - 1), \quad (13)$$

where d_1 = density of the solvent (g/cm³), \bar{v}_2 = partial specific volume of the solute (cm³/g).

Assuming the volume, which has been calculated from the invariant, and ϕ'_2 instead of \bar{v}_2 , we find for the enzyme core complex $x = 1.03$ g solvent/g protein. This value for x is — as compared with the solvent content of other enzymes of about $x = 0.3$ g/g found by the X-ray small-angle technique — very high, but can easily be explained. A multienzyme complex *loosely* built up from many subunits possesses a lot of cavities within the molecule and therefore a high degree of solvent included in the assembly of subunits.

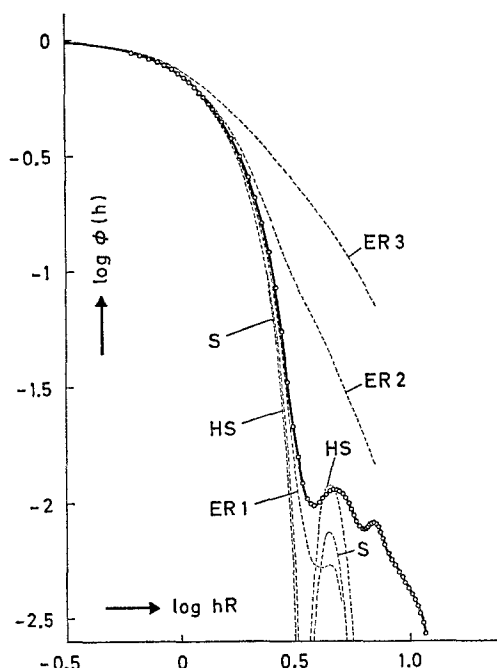
But, the packing of subunits must be other than in the multienzyme complex of fatty acid synthetase, where also a small value for x of 0.22 g/g was found by means of an X-ray small-angle study (Pilz *et al.*, 1970). In this latter multienzyme complex the disperse phase of the molecule, represented by the subunits, has to be relatively closely connected. The subunits of fatty acid synthetase are assembled in form of a well-defined, nearly spherical shell divided in half by a planar wall and with large hollow spaces inside (whereby large holes do not contribute to V_{exp}). Moreover, this result was confirmed by the authors by determining the wall thickness of the shell according to Porod (1949). On the other hand, the special architecture of loosely packed subunits in the pyruvate dehydrogenase complex was established by the lack of such a thickness factor, by the high value for x , as well as by determination of characteristic structural numbers and model calculations concerning shape and arrangement of subunits in the complex as will be shown in Part II of this investigation.

Overall Shape of the Particle

The comparison between experimental and theoretical scattering curves yields information about shapes, which are equivalent in scattering (Kratky and Porod, 1948; Porod, 1948; Mittelbach and Porod, 1961, 1962; Mittelbach, 1964). For this purpose we use the double logarithmic plot of $\log \phi(h)$ versus $\log hR$.

As a first approach, the experimental scattering curve was compared with theoretical scattering curves of simple full and hollow bodies of various geometry and of various axial and hollow space ratios. Fig. 6 delivers a short selection out of a large variety of comparisons of scattering curves of such kind. The comparisons establish that the anisometry of the molecule is not too large, as is shown by the comparison with the anisometric ellipsoids of revolution ER 2 and ER 3 on the one hand, and the relatively isometric ellipsoid of revolution ER 1 and the sphere S or hollow sphere HS on the other. But, and we should stress this point, there is not even a rough conformity in the course of the outer part of the scat-

Fig. 6. Log-log plot for comparison of the experimental scattering curve (○) of the enzyme core complex with theoretical scattering curves of simple full and hollow bodies. S, sphere; HS, hollow sphere of radius ratio $r_i/r_o = 0.3$; ER 1, ER 2, ER 3, ellipsoids of revolution of axial ratio $a:b:c = 2/3:1:1$ or $0.1:1:1$ or $10:1:1$. No satisfactory agreement between experimental and theoretical scattering curves in the range of the submaxima was obtained



tering curves. The most outstanding feature is the high scattering intensity in the angular range of the second and third submaximum, while the high intensity of the first submaximum may be interpreted in terms of hollow spaces within the molecule, as is shown, for example, by the comparison with the hollow sphere HS of the axial ratio of $r_i/r_o = 0.3$. The absence of ideal spherical symmetry can be shown by the absence of zero positions in the experimental scattering curve, but which are present in the theoretical ones of the sphere S or the hollow sphere HS.

The aim of additional calculations of theoretical scattering curves will be to comment on the special course of the experimental scattering curve in the range of the submaxima. The calculation of theoretical scattering curves of bodies built up from subunits of different size and arrangement should be able to clear up this point.

The structure of the core complex could be crudely pictured as a loose assembly of subunits arranged in such a way as to form a relatively isometric complex with slightly disturbed spherical symmetry. Additional information about the shape of the particle may be gained from the radial excess electron density distribution, from the statistic of intersects, and by determination of further structural parameters characterizing the fine structure of the complex. By means of an educated guess based on all structural parameters, obtained from the scattered intensity and the Fourier transformed functions, we should be able to carry out detailed model calculations and to propose a definite model for the arrangement of subunits in the core complex. This topic will be dealt with in Part II: Subunit Structure of the Core Complex in a subsequent paper in this journal.

Acknowledgements. The author expresses gratitude to Professor Dr. Dr. h.c. Otto Kratky, in whose laboratory in Graz the work was carried out, for his kind interest in the problem. The author is much indebted to Dr. Peter Zipper, Graz, for helpful and stimulating discussions. Part of the evaluation work was done during a stay in Professor Dr. Rainer Jaenicke's biochemical group in Regensburg. This stay was made possible by an EMBO long-term fellowship awarded to the author. Sincerest thanks are also due to Professor Dr. Ulf Henning and Dr. Otto Vogel from the Max-Planck-Institut für Biologie, Tübingen, for the generous gift of the enzyme and the determination of protein concentration.

Calculations were performed on a UNIVAC 494 computer in the Rechenzentrum Graz and on a SIEMENS 4004/45-G computer in the Rechenzentrum Universität Regensburg.

References

- Beisenherz, G., Boltze, H. J., Bücher, Th., Czok, R., Garbade, K. H., Meyer-Arendt, E., Pfeleiderer, G.: Diphosphofructose-Aldolase, Phosphoglyceralddehyd-Dehydrogenase, Milchsäure-Dehydrogenase, Glycerophosphat-Dehydrogenase und Pyruvat-Kinase aus Kaninchenschmuskulatur in einem Arbeitsgang. *Z. Naturforsch.* **8b**, 555—577 (1953)
- Debye, P., Bueche, A. M.: Scattering by an inhomogeneous solid. *J. appl. Phys.* **20**, 518—525 (1949)
- Dennert, G., Höglund, S.: Pyruvate dehydrogenase of *Escherichia coli* K 12. *Europ. J. Biochem.* **12**, 502—507 (1970)
- Durchschlag, H.: Röntgenkleinwinkeluntersuchungen am *E.-coli*-Pyruvat-Dehydrogenase-Core-Komplex. Abstr. Wintertag. Ges. Biol. Chem., Konstanz 1973. *Hoppe-Seylers Z. physiol. Chem.* **354**, 205—206 (1973)
- Durchschlag, H.: X-ray small-angle studies of the pyruvate dehydrogenase core complex from *Escherichia coli* K-12. Abstr. 3rd Int. Conf. on X-ray and neutron small-angle scattering, Grenoble 1973, *J. appl. Cryst.* **7**, 167 (1974)
- Durchschlag, H., Puchwein, G., Kratky, O., Schuster, I., Kirschner, K.: X-ray small-angle scattering of yeast glyceraldehyde-3-phosphate dehydrogenase as a function of saturation with nicotinamide-adenine-dinucleotide. *Europ. J. Biochem.* **19**, 9—22 (1971)
- Eley, M. H., Namihiro, G., Hamilton, L., Munk, P., Reed, L. J.: α -Keto acid dehydrogenase complexes. XVIII. Subunit composition of the *Escherichia coli* pyruvate dehydrogenase complex. *Arch. Biochem. Biophys.* **152**, 655—669 (1972)
- Flatgaard, J. E., Hoehn, B., Henning, U.: Mutants of *Escherichia coli* K-12 which synthesize the pyruvate dehydrogenase complex constitutively. *Arch. Biochem. Biophys.* **143**, 461—470 (1971)
- Guinier, A.: La diffraction des rayons X aux très petits angles: application à l'étude de phénomènes ultramicroscopiques. *Ann. phys.* **12**, 161—237 (1939)
- Guinier, A., Fournet, G.: Facteurs de correction dans les mesures de la diffusion des rayons X aux faibles angles. *J. Phys. Radium (Paris)* **8**, 345—351 (1947)
- Gunsalus, I. C.: In: A symposium on the mechanism of enzyme action (eds. W. D. McElroy, B. Glass), pp. 545—577. Baltimore: The Johns Hopkins Press 1954
- Heine, S.: Die Entschmierung von Röntgen-Kleinwinkel-Streukurven mit einer elektronischen Rechenanlage. *Acta Phys. Austriaca* **16**, 144—158 (1963)
- Heine, S., Roppert, J.: Die Behandlung des Problems der Entschmierung von Röntgen-Kleinwinkel-Streukurven mittels einer elektronischen Rechenanlage. *Acta Phys. Austriaca* **15**, 148—166 (1962)
- Henning, U., Vogel, O., Busch, W., Flatgaard, J. E.: The pyruvate dehydrogenase complex of *E. coli* K-12. Structure and synthesis. In: Protein-protein interactions, 23rd Mosbach Colloquium (eds. R. Jaenicke, E. Helmreich), pp. 343—364. Berlin-Heidelberg-New York: Springer 1972
- Kirste, R., Porod, G.: Röntgenkleinwinkelstreuung an kolloiden Systemen. Asymptotisches Verhalten der Streukurven. *Kolloid-Z.* **184**, 1—7 (1962)
- Koike, M., Reed, L. J., Carroll, W. R.: α -Keto acid dehydrogenation complexes. IV. Resolution and reconstitution of the *Escherichia coli* pyruvate dehydrogenation complex. *J. biol. Chem.* **238**, 30—39 (1963)
- Kratky, O.: Neues Verfahren zur Herstellung von blendenstreuungsfreien Röntgen-Kleinwinkel-aufnahmen. *Z. Elektrochem.* **58**, 49—53 (1954)

- Kratky, O.: X-ray small angle scattering with substances of biological interest in diluted solutions. *Progr. Biophys. molec. Biol.* **13**, 105—173 (1963)
- Kratky, O.: Die Messung der Absolutintensität der diffusen Röntgenkleinwinkelstreuung — ein Verfahren zur „Wägung“ in makro-molekularen Systemen. *Z. anal. Chem.* **201**, 161—194 (1964)
- Kratky, O.: Adaptation of the technique of diffuse small-angle X-ray scattering to extreme demands. In: *Small-angle X-ray scattering*, Proc. Conf. at Syracuse University 1965 (ed. H. Brumberger), pp. 63—120. New York, London, Paris: Gordon and Breach 1967
- Kratky, O., Leopold, H., Stabinger, H.: Dichtemessungen an Flüssigkeiten und Gasen auf 10^{-6} g/cm³ bei 0,6 cm³ Präparatvolumen. *Z. angew. Physik* **27**, 273—277 (1969)
- Kratky, O., Pilz, I.: Recent advances and applications of diffuse X-ray small-angle scattering on biopolymers in dilute solutions. *Quart. Rev. Biophys.* **5**, 481—537 (1972)
- Kratky, O., Pilz, I., Schmitz, P. J.: Absolute intensity measurement of small angle X-ray scattering by means of a standard sample. *J. Colloid Interface Sci.* **21**, 24—34 (1966)
- Kratky, O., Porod, G.: Die Abhängigkeit der Röntgen-Kleinwinkelstreuung von Form und Größe der kolloiden Teilchen in verdünnten Systemen, III. *Acta Phys. Austriaca* **2**, 133—147 (1948)
- Kratky, O., Porod, G., Kahovec, L.: Einige Neuerungen in der Technik und Auswertung von Röntgen-Kleinwinkelmessungen. *Z. Elektrochem.* **55**, 53—59 (1951)
- Kratky, O., Porod, G., Skala, Z.: Verschmierung und Entschmierung bei Röntgen-Kleinwinkeldiagrammen. *Acta Phys. Austriaca* **13**, 76—128 (1960)
- Kratky, O., Skala, Z.: Neues Verfahren zur Herstellung von blendenstreuungsfreien Röntgen-Kleinwinkel-aufnahmen, V. *Z. Elektrochem.* **62**, 73—77 (1958)
- Kupke, D. W.: Density and volume change measurements. In: *Physical Principles and Techniques of Protein Chemistry*, part C (ed. S. J. Leach), pp. 1—75. New York: Academic Press 1972
- Leopold, H.: Elektronische Programmierereinrichtung zur Vermessung von Röntgenkleinwinkelstreu曲ven. *Z. angew. Physik* **25**, 81—85 (1968)
- Leopold, H.: Peltier-Thermostat kühlt oder heizt automatisch. *Elektronik* **18**, 350—351 (1969)
- Luzzati, V., Witz, J., Nicolaieff, A.: Détermination de la masse et des dimensions des protéines en solution par la diffusion centrale des rayons X mesurée à l'échelle absolue: exemple du lysozyme. *J. molec. Biol.* **3**, 367—378 (1961)
- Mittelbach, P.: Zur Röntgenkleinwinkelstreuung verdünnter kolloider Systeme VIII. Diskussion des Streuverhaltens regelmäßiger Körper und Methoden zur Bestimmung von Größe und Form kolloider Teilchen. *Acta Phys. Austriaca* **19**, 53—102 (1964)
- Mittelbach, P., Porod, G.: Zur Röntgenkleinwinkelstreuung verdünnter kolloider Systeme. Die Berechnung der Streukurven von Parallelepipeden. *Acta Phys. Austriaca* **14**, 185—211 (1961); Zur Röntgenkleinwinkelstreuung verdünnter kolloider Systeme VI. Die Berechnung der Streukurven von elliptischen Zylindern und Hohlzylindern. *Acta Phys. Austriaca* **14**, 405—439 (1961); Zur Röntgenkleinwinkelstreuung verdünnter kolloider Systeme VII. Die Berechnung der Streukurven von dreiachsigen Ellipsoiden. *Acta Phys. Austriaca* **15**, 122—147 (1962)
- Perham, R. N., Thomas, J. O.: The subunit molecular weights of the α -keto acid dehydrogenase multienzyme complexes from *E. coli*. *FEBS-Lett.* **15**, 8—12 (1971)
- Pilz, I.: Absolute intensity measurement of small-angle X-ray scattering by means of a standard sample, III. *J. Colloid Interface Sci.* **30**, 140—144 (1969)
- Pilz, I., Herbst, M., Kratky, O., Oesterhelt, D., Lynen, F.: Röntgenkleinwinkel-Untersuchungen an der Fettsäuresynthetase aus Hefe. *Europ. J. Biochem.* **13**, 55—64 (1970)
- Pilz, I., Kratky, O.: Absolute intensity measurement of small-angle X-ray scattering by means of a standard sample, II. *J. Colloid Interface Sci.* **24**, 211—218 (1967)
- Porod, G.: Die Abhängigkeit der Röntgen-Kleinwinkelstreuung von Form und Größe der kolloiden Teilchen in verdünnten Systemen, IV. *Acta Phys. Austriaca* **2**, 255—292 (1948)
- Porod, G.: Theorie der diffusen Röntgenkleinwinkelstreuung an kolloiden Systemen. *Z. Naturforsch.* **4a**, 401—414 (1949)
- Porod, G.: Die Röntgenkleinwinkelstreuung von dichtgepackten kolloiden Systemen, I. Teil. *Kolloid-Z.* **124**, 83—114 (1951); Die Röntgenkleinwinkelstreuung von dichtgepackten kolloiden Systemen, II. Teil. *Kolloid-Z.* **125**, 51—57 and 108—122 (1952)

- Porod, G.: Determination of general parameters by small-angle X-ray scattering. In: Small-angle X-ray scattering, Proc. Conf. at Syracuse University 1965 (ed. H. Brumberger), pp. 1—15. New York, London, Paris: Gordon and Breach 1967
- Reed, L. J., Leach, F. R., Koike, M.: Studies on a lipoic acid-activating system. J. biol. Chem. **232**, 123—142 (1958)
- Reed, L. J., Oliver, R. M.: The multienzyme α -keto acid dehydrogenase complexes. Brookhaven Symp. Biol. **21**, 397—412 (1968)
- Sloan, D. L., Velick, S. F.: Protein hydration changes in the formation of the nicotinamide adenine dinucleotide complexes of glyceraldehyde 3-phosphate dehydrogenase of yeast. I. Buoyant densities, preferential hydrations, and fluorescence-quenching titrations. J. biol. Chem. **248**, 5419—5423 (1973)
- Vogel, O., Beikirch, H., Müller, H., Henning, U.: The subunit structure of the *Escherichia coli* K-12 pyruvate dehydrogenase complex. The dihydrolipoamide transacetylase component. Europ. J. Biochem. **20**, 169—178 (1971)
- Vogel, O., Henning, U.: Pyruvate dehydrogenase component subunit structure of the *Escherichia coli* K-12 pyruvate dehydrogenase complex. Europ. J. Biochem. **18**, 103—115 (1971)
- Vogel, O., Henning, U.: The subunit structure of the *Escherichia coli* K 12 pyruvate-dehydrogenase complex. Dihydrolipoamide-dehydrogenase component. Europ. J. Biochem. **35**, 307—310 (1973)
- Vogel, O., Hoehn, B., Henning, U.: The subunit structure of the pyruvate-dehydrogenase complex from *Escherichia coli* K-12. The core complex. Europ. J. Biochem. **30**, 354—360 (1972a)
- Vogel, O., Hoehn, B., Henning, U.: Molecular structure of the pyruvate dehydrogenase complex from *Escherichia coli* K-12. Proc. nat. Acad. Sci. (Wash.) **69**, 1615—1619 (1972b)
- Zipper, P.: Ein einfaches Verfahren zur Monochromatisierung von Streukurven. Acta Phys. Austriaca **30**, 143—151 (1969)
- Zipper, P.: The evaluation of small-angle X-ray scattering data by a computer. Acta Phys. Austriaca **36**, 27—38 (1972)

Dr. Helmut Durchschlag
Biochemie II, Fachbereich Biologie
Universität Regensburg
D-84 Regensburg
Federal Republic of Germany